BULLETIN OF THE POLISH ACADEMY OF SCIENCES
TECHNICAL SCIENCES, Vol. 66, No. 3, 2018
DOI: 10.24425/123439

Sintered nanosilver joints on rigid and flexible substrates

K. KIEŁBASIŃSKI[2], J. SZAŁAPAK[3], A. MŁOŻNIAK[1], M. TEODORCZYK[1], R. PAWŁOWSKI[4], J. KRZEMIŃSKI[3], and M. JAKUBOWSKA[3]

[1]Institute of Electronic Materials Technology, Wólczyńska 133, 01-919 Warsaw, Poland
[2]Warsaw University of Technology, Institute of Microelectronics and Optoelectronics, Koszykowa 75, 00-662 Warsaw, Poland
[3]Warsaw University of Technology, Faculty of Mechatronics, Św. Andrzeja Boboli 8, 02-525 Warsaw, Poland
[4]Abraxas, ul. Piaskowa 27, 44-300 Wodzisław Śląski, Poland (abraxas@abraxas.com.pl)

Abstract. Because of new EU laws restricting the use of harmful substances (i.e. Pb because of the RoHS Directive), the search for new methods of joining electronics has become highly urgent. The main problem for most solutions known to date has been to achieve good electrical parameters while maintaining low sintering temperatures. Pastes based on silver nanoparticles were developed, which allow to sinter below 300°C. Those layers have sheet resistance below 2 mΩ/sq. Low exposure to heat allows to use these pastes on elastic substrates such as paper or Kapton foil. In present work, the authors proved that it is possible to obtain joints on elastic substrates which can withstand over 30 000 cycles in bend test, with sintering in 300°C, by means of the Low Temperature Joining Technique (LTJT).

Key words: silver nanopowder, pressure sintering, thermal conductivity.

1. Introduction

Standard packaging and interconnection technologies of power devices have difficulties meeting the increasing thermal demands of new application fields of power electronic devices. Decreasing reliability of bond-wires and solder layers combined with increasing junction temperature constitute the main restrictions [1]. The attractiveness of using silicon carbide for high power and high temperature electronics is yet another driver for developing new die-attachment technologies. The method used for joining dies with chip carriers is crucial for device reliability. Such interfaces need to be mechanically reliable and to have high coefficient of thermal expansion in order to effectively retrieve heat from the chip. High coefficient value is not the sole important factor. It has to match factors of other system components. i.e. the chip and substrate. Such fitting reduces tensions in the system [2].

Operating temperature of traditional soldered power electronics packages and modules is limited to around 150°C or even below this temperature, because solder alloys find their melting points around 220°C. Devices with such bonding materials cannot meet the requirements of next-generation power electronics applications [3]. Predominantly, the bonding layers should:

- not transmit destructive stresses to dies during bonding and operation,
- withstand extreme temperatures without degradation of bonding quality,

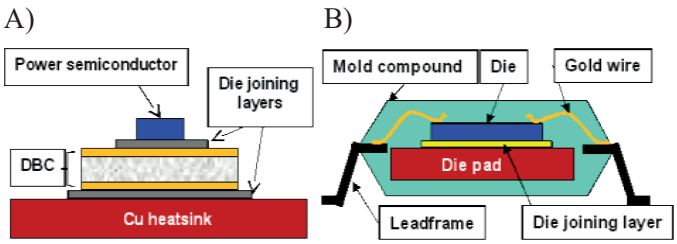

Fig. 1. Bonding layer location in A) high power, and B) low cost plastic electronic packages

- provide good electrical and thermal contact between a die and substrate.

Typical locations of bonding layers in a high power package and a low cost package are shown in Fig. 1.

Silver was proposed as the joining material to face these problems. It is substantially cheaper than gold and palladium. Its melting point stands at 961°C and it can work in much higher temperatures than solders, which is crucial for device reliability. Silver has significantly better electrical and thermal conductivity and a lifetime that is several-fold longer than solders during temperature cycling [4]. A sintered Ag layer has up to five times higher electrical conductivity and about four times higher thermal conductivity as compared to SnAg or SnPb solder layers. This is shown in Table 1.

Additionally, there are several EU Directives which aim to restrict the use of certain hazardous substances, including lead, in electrical and electronic equipment. Those include e.g. the RoHS (Restriction of Hazardous Substances) Directive. The Pb-Sn alloy used as the die-attach material is exempted from these Directives until 2014 but it is hard to find a lead-free replacement. Current candidates, such as the Bi-, Zn- or Au-Sn

*e-mail: k.kielbasinski@imio.pw.edu.pl

Manuscript submitted 2016-09-14, revised 2017-05-15 and 2017-09-22, initially accepted for publication 2017-10-19, published in June 2018.

Table 1
Comparison of properties of different joining methods

Joining material	Process temp. [°C]	Working temp. [°C]	Electrical cond.* 10^7 [$\Omega^{-1}m^{-1}$]	Thermal cond. [W/K*m]	Shear Strength [MPa]
Tin lead solders [6]	217	<92	0.69	~50	20–30
Lead-free solder (SAC 305) [6]	260	<125	0.80	~70	25–35
Gold-tin solder [7]	330	<185	0.61	~57	30–60
Conductive adhesives [8]	100–200	<200	<0.1	1.3–3.1	10–20
Silver sintered joints (LTJT) [9–10]	~300	<715	3–4	150–250	25–35

alloys, are costly and have other limitations, such as poor processability and corrosion resistance [5].

There are some other drawbacks as well. Silver layers are not susceptible to oxidation problems as compared to other metals. Commonly used silver pastes, containing the functional and glassy phase, need to be sintered at high temperatures (>600°C), in contrast with reflow soldering. Pressure-assisted sintering enables to lower the sintering temperature, but it provides stresses to the system. Glass remaining in the sintered layer causes lower electrical and thermal properties and softens under high temperatures (300–400°C), causing layer instability. These facts exclude the use of such materials for high temperature applications.

The Low Temperature Joining Technique (LTJT) is generally regarded as an alternative to lead-free die-attach for high power and high temperature applications [11–12]. It started with micron-scale Ag pastes. The flake powder was preferred due to sinterability in temperatures as low as 200°C [13], however high sintering pressure of even 30 MPa was still necessary to form reliable joints. In order to reduce the pressure required during sintering, Ag particles of nanometer size can be used. When reduced to such dimension, the effective surface area increases. This causes an increase in surface curvature which provides driving forces to sinter with neighboring atoms at temperatures 0.2–0.4 off silver's melting point [3]. Different paste compositions and processing parameters such as pressure, temperature and time also affect joint porosity and mechanical properties of silver joints [14–16].

The sintering properties of fine powders have made pressure-less joining possible. However the electrical and mechanical properties of these joints are inferior to those obtained with pressure assistance [17–18].

The authors have been studying conductive thick-film pastes based on micro-scale silver powders for several years now, establishing their complex technology. These pastes have existed in the market for many years. Standard thick-film silver pastes contain silver grains or flakes, glass frit, resin and solvents. Then, the authors elaborated and presented novel thick-film, conductive pastes designed for screen printing and firing containing only silver-nanoparticle powder and an organic carrier [19]. Sintering temperature decreased and performance under high temperature and high current stress increased. Such materials, capable of high temperature and power, may be used as conductors for carrying signals from chips in ceramic packages of contemporary electronic circuits. Now, the idea is to use similar pastes as die-attach materials in electronic packaging.

There is also strong demand to integrate electronic circuits with everyday use consumer goods such as clothes, books and other elastic things in other areas, which should not be dominated by rigid circuits. This demand can be met by emerging elastic electronics which include materials and depositing methods suitable for elastic substrates. The development of paper-, foil- and textile-compatible materials is still on the way. Elastically active organic devices still have properties inferior to the silicon-based ones. In the case of complex electronic devices, this can be a serious limitation. The ideal solution is to integrate complex silicon devices into elastic circuits. Therefore there is also a need to join silicon active dies with elastic circuits.

2. Materials

2.1. Paste. Pastes with silver nanoparticles and silver flakes were prepared for the experiment. Mixing the large particles with the nanoparticles allows to obtain higher packing density than that arrived at by means of applying mono-sized particles. For spherical particles geometrical packing density is 0.74. By mixing two powders with more than 10 times the aspect ratio, packing density can be theoretically raised up to 0.9324. The mixing ratio for fine to large particles equaled 0.26/0.74.

Samples of silver nanopowders used in the experiment were elaborated by Helioenergia Ltd [20] based on the license supplied by the Institute of Electronic Materials Technology and the Warsaw University of Technology. Silver flakes were the AX20LC variety, obtained from Amepox. Their average diameter was 4–10 μm and the thickness was around 100 nm. The powders were mixed in the ratio of 1:3 small to large particles.

Silver nanoparticles were obtained from fat acids (palmitic) with silver salt by means of thermal decomposition in an atmosphere of nitrogen. Palmitic salt decomposition gives average grain size of 7 nm with standard deviation of 5.4 nm, as shown in Fig. 2. Nanoparticles are protected against room temperature sintering by a 20–25% ratio of palmitic acid chains acting as an

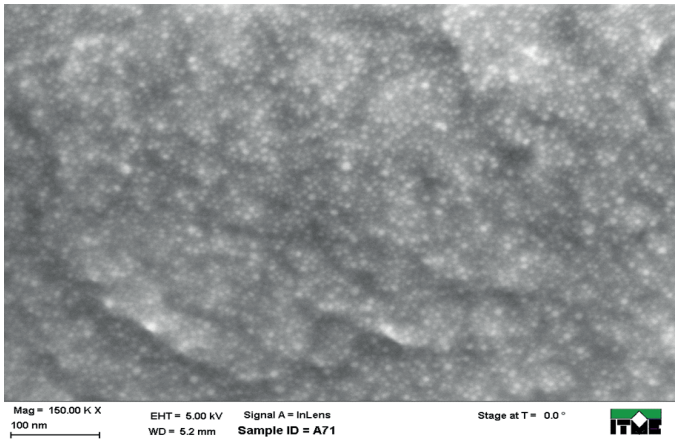

Fig. 2. SEM photograph of silver nanoparticles

organic coating. As a vehicle for the paste, Polymethyl methacrylate 8% wt. in a butyl carbitol acetate solution was used.

2.2. Substrates. Materials containing silver nanoparticles have the unique property of adhering to many substrates without the necessity of grass frit or spinel forming compounds. That provides for an opportunity to create paths that are very effective at conducting and resistant to high temperatures, and that adhere to many rigid substrates used in electronics without any interlayers such as alumina, glass, bare aluminum, copper or gold. However it has been discovered that voids can be formed between a silver joint and a gold-plated pad, resulting in reduced mechanical strength. This problem usually arises after aging [21–22].

Elastic polyimide foil can also be used, due to fact that its sintering temperature does not exceed 300°C. Examples of conductive silver paths glass and polyimide substrates are shown in Fig. 3. The LTJT method is suitable for joining silicon dies with gold or silver metallization. In this paper two group of substrates were used: rigid and flexible ones. The first was a 0.8 mm thick copper plate with silver plating and the second was a 0.076 mm polyimide foil. The polyimide foil was covered with thick-film nanoparticle silver conductive paths containing the silver described herein.

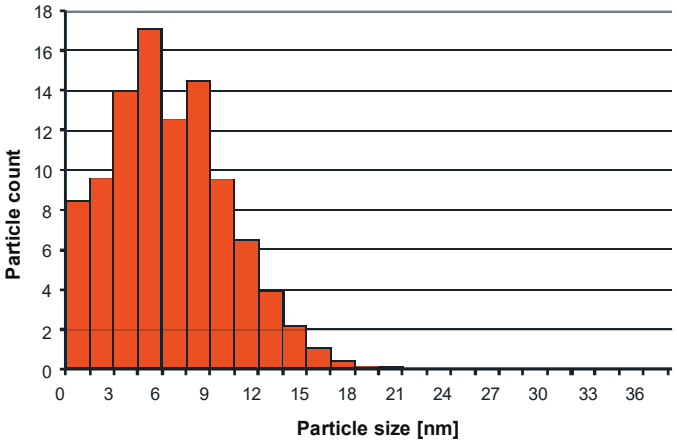

Fig. 3. Silver grain size distribution

3. Sample preparation

3.1. Printing. The test pattern on isolating substrate, including ceramic, glass and polyimide, contains the conductive electrical circuit and a joint.

Two different methods of printing were applied for them. Creating a conductive pattern by means of screen printing is preferred due to fact that it allows to create closed loops and other complicated shapes. However, screen printing of nanomaterials results in considerable surface roughness, of more than 5 microns, which is not suitable for a die attachment. Therefore, the paste under a joined component was deposited by a stencil printing a layer that was 100 microns thick. Thickness of the deposited layer was around 80 microns.

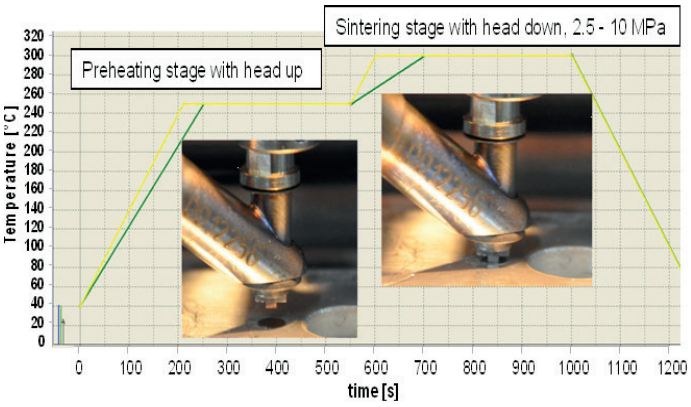

Fig. 4. Temperature ramp during sintering process

After the printing and prior to sintering, a 15 minutes in 120°C was allowed for drying. Nanomaterials usually have a higher content of organics, as compared to micro materials, therefore that step is essential. After printing, the conductive circuits can be sintered in a chamber furnace for 30–60 minutes at 250–300°C. Finally, the joining pad was covered with paste and dried in the conditions as described above.

The joining procedure was conducted by means of a thermocompression method with the use of a Finetech Micro fineplacer. The joining procedure consists of two main steps as shown in Fig. 5. The first is conducted with the vacuum head in the upper position, and can be regarded as a continuation of the drying procedure at the 60°C/min. ramp with a 5-minute dwell time at 250°C. This allows organic vehicles to evaporate entirely. In the next step, the head with the component being held is lowered, and the component is pressed towards the substrate with the silver-based layer on it. The temperature is raised to

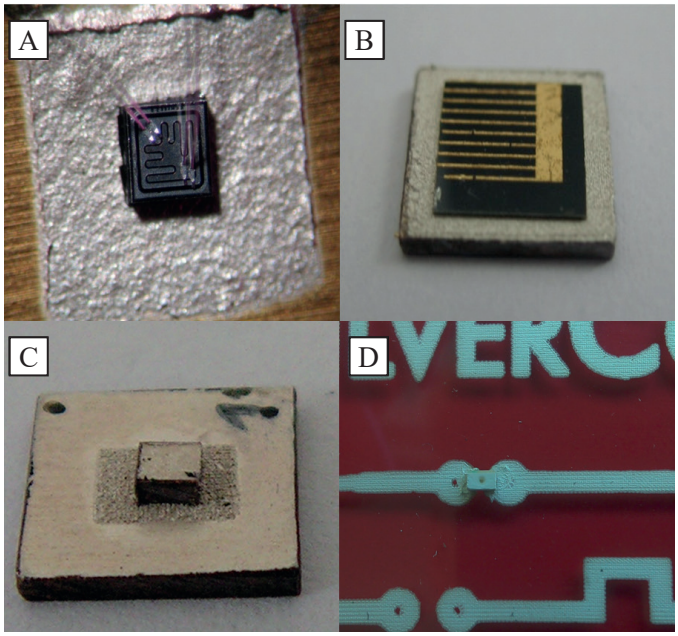

Fig. 5. A) power BJT, B) photovoltaic module, C) dummy die joined with silvered copper, and D) LED structure joined with silvered glass

300°C, where the sintering process starts. Due to the sintering, the silver nanoparticles connect with each other, growing into a bulk layer. Ventilation of the joint is then very limited, therefore high content of organics left during the previous step would only cause gassing, which disturbs sintering of silver particles and increases joint porosity. After sintering, natural cooling is performed, with the temperature falling to 60°C. Final joint thickness drops to around 30 microns.

Many types of structures can be joined. This includes active structures, like power transistors (Fig. 5A), laser diodes, LED devices and photovoltaic 5×5 mm modules (Fig. 5B). The active devices are not convenient for electrical thermal and mechanical joint characterization therefore on some samples dummy dies were applied instead (Fig. 5C). Dummy dies were cut out from a plain copper plate of 0.8 mm in thickness into the square shape of 2×2 mm. The surface of the dummy chip was electroplated with silver to avoid copper oxidation.

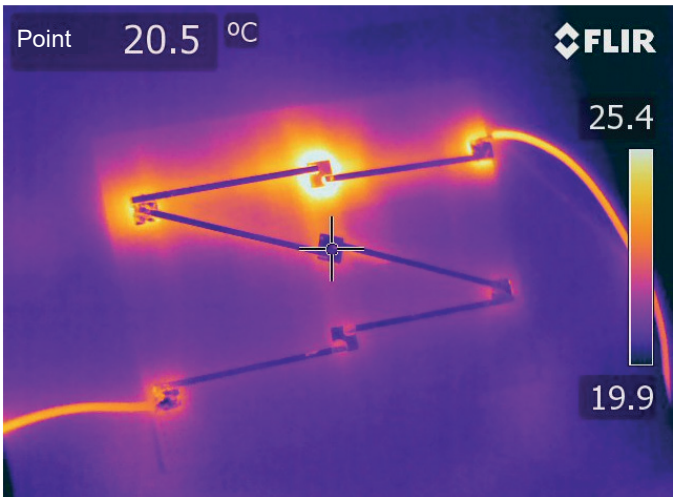

Fig. 7. Temperature comparison of three joining techniques with thermal imaging

4. Test procedure and results

The joints were investigated by means of several tests. The dummy dies on a rigid substrate were tested electrically, thermally and finally electrically.

4.1. Thermal investigation. Thermal evaluation was carried out by two methods. The first one was based on a comparison of Joule heat of the silver joint with other joining technologies, including soldering with an SnPb compound and a conductive adhesive. The daisy-chain of silver plated copper conductors was formed (Fig. 6) and constant current load was applied. The joints were observed by means of the thermal imaging method (Fig. 7) after applying a graphite spray, which rises the emission coefficient. The higher the resistance of the joint, the higher the Joule heat generated and therefore the higher the resulting temperature.

The temperature readout was taken once the heat transfer to the ambient had stabilized. The ambient temperature was 19.9°C. The temperature readouts of three components joined with three different materials are shown in Table 2. Due to quite a low temperature gradient between component temperature and the ambient (less than 6°C), the black body irradiation can be neglected, so the temperature gradients of the joints are closely proportional to Joule heat.

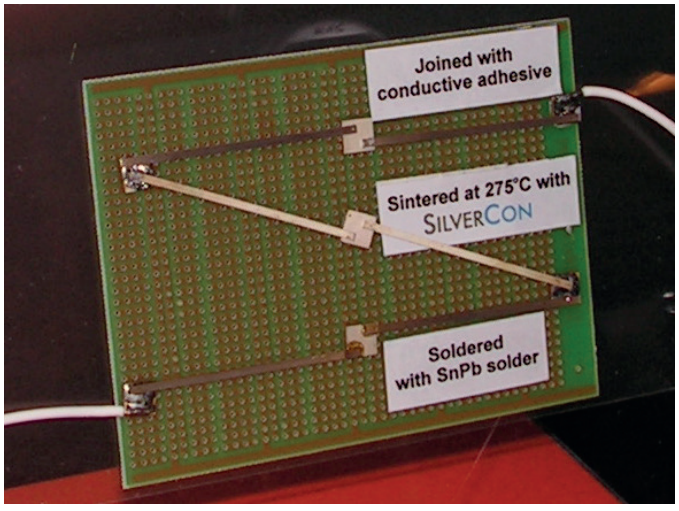

Fig. 6. Bar-plate daisy chain made with three joining techniques

Table 2
Temperature readouts and gradients of components joined with different methods

Joining material	Temp. of component [°C]	Temp. gradient component-ambient [°C]	Rel. Joule heat [a.u]
Silver based conductive adhesive	20.5	5.5	9.2
SnPb solder	21.6	1.7	2.8
LTJT joint	25.4	0.6	1

The sintered joint dissipates 2.8 times less heat than the soldered one and 9.2 times less than the adhesive bonded joint. Joule heat is proportional to joint resistance, therefore ratios of Joule heat and resistance of different joints are similar.

For the second method, Laser Flash Analysis. Netzsch LFA 457 microflash was used for samples shown in Fig. 5C. The results of the measurements were processed by bundled Netzsch software and the given thickness of the layers resulted in the heat conductivity of a joint at 141 W/mK. Due to fact that the cross section of the top of the sample is smaller than that of the bottom of the sample, the effective heat travel distance is larger than the total sample height. This cannot be considered when using Netzsch software, which leads to serious underestimation of heat diffusivity and derived heat conductivity. The detailed method of compensation for that mismatch was described in [7]. For the applied geometry of the tested sample the effective heat travel length is larger by a factor of 1.17 than it would have been for a rectangular sample. According to the Parker's for-

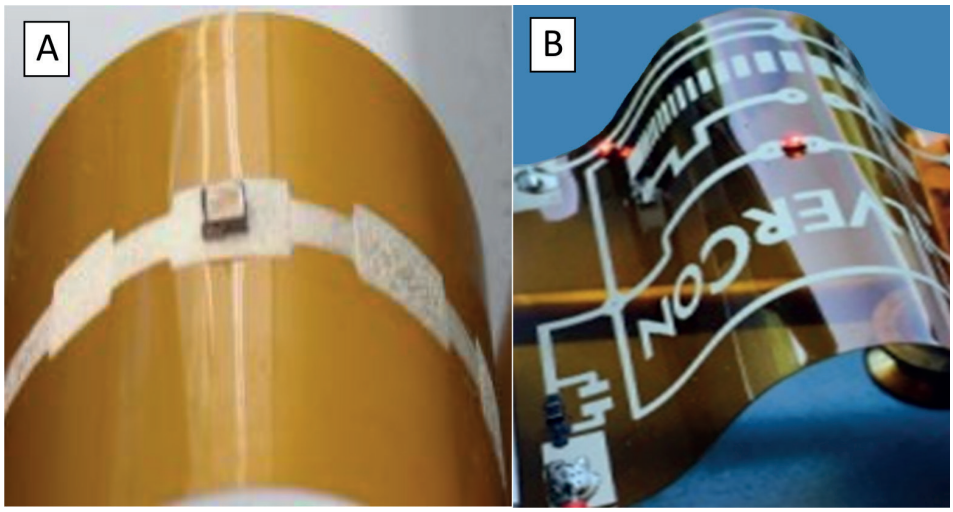

Fig. 8. Bend test of A) dummy die, and B) LED components on polyimide elastic foil

mula, this translates into underestimation of heat conductivity by a factor of $(1.17)^2$. Therefore new compensated value of heat conductivity of a joint is 193 W/mK, i.e. about 3 times more than for SnPb solders. That is consistent with the temperature rise in the daisy chain tested with the current load method.

4.2. Electrical investigation. Electrical measurements were made on test structures on rigid silvered copper structures and on flexible substrates shown in Fig. 8A. During resistance measurements on rigid substrate, the current flowed through the whole sandwich from two multi pin coaxial probes, one on the bottom and one on the top of the sandwich. The current flow was not perfectly vertical, due to a mismatch in the sizes of plate and die and the finite number of current pins in the probes. The results measured also contain the resistance components from substrate joint and dummy die. To extract joint contact resistivity from the total resistance value, the current flow model was analyzed. Details of the resistivity measurements method are described in [8]. The results of electrical measurement are presented in Table 3.

Table 3
Properties of joint area

Property	Value
Largest pore diameter [mm]	0.179
Average pore diameter [mm]	0.0633
Mean pore area [mm^2]	0.000906
Porosity	16.8%
Contact resistivity [$\Omega*m^2$]	$1.89*10^{-12}$
Joint thickness [μm]	30
Joint resistivity [Ω*m]	$6.3*10^{-8}$

4.3. Mechanical investigation. Samples on elastic substrates were treated mechanically using a cyclic bend test. Polyimide foil of 0.076 mm in thickness was used. Two kind of samples were tested. One with the dummy die and the other with commercial 0805 LED components intended for surface mounting by means of lead-free soldering. The testing machine has two handles, one of which is stationary while the second one moves in a reciprocating movement towards and away, thereby bending and straightening the tested element (Fig. 8B). The machine provides a changing bending radius, from infinity to about 6 mm during each cycle. The samples were mounted in such a way that the dummy chip was exactly between the holders, and therefore in the middle of the bend. The speed was set at maximum, i.e. 300 cycles/min. Just like in the first test, electrical resistance was measured after every 1 000 cycles. The stress calculated during the bending test equals 18.82 MPa. The electrical resistance measured in the 7A setup was below 20 μΩ and remained the same after 10 000 bending cycles within 1% of measuring accuracy. The sample with LED components was constantly powered during the test. No flickering was observed during bending or straightening even after 10 000 cycles. The joint quality of 8 samples was investigated by each bend test. The first testing machine (CR) allowed to examine the impact of the slide across the sample with constant radius inflection. The tested element is mounted in two brackets at different heights, the top of which is stationary while the lower moves. Bend radius can be regulated with changing the height of the top one – the radius chosen for this study was 6 mm. The speed was set at maximum, i.e. 250 cycles/min. Electrical resistance was measured after every 1 000 cycles.

During bending of the substrate compressive strain appears on the inner side of the substrate while tensile strain can be observed on the outer side of the substrate, as shown in Fig. 6.

The strain ε on the surface of bended foil with the given thickness h and bending radius R can be calculated by means of the following formula:

$$\varepsilon = \ln\left[\frac{1}{\frac{2R}{h}+1}+1\right]. \tag{1}$$

For 0.076 mm of substrate thickness and 6 mm of bending radius that gives strain equal to $\varepsilon = 6274$ ppm. Stress in the area of the joint can be calculated by multiplying Young's modulus of the substrate (3 GPa) by the strain value, i.e.:

$$\sigma = E * \varepsilon. \tag{2}$$

During bending of the substrate compressive strain appears on the inner side of the substrate while tensile strain can be observed on the outer side of the substrate.

The SEM picture of the side following the bending test (Fig. 9) revealed delamination at the edges of the dummy die. However, this process did not progress any further under the die.

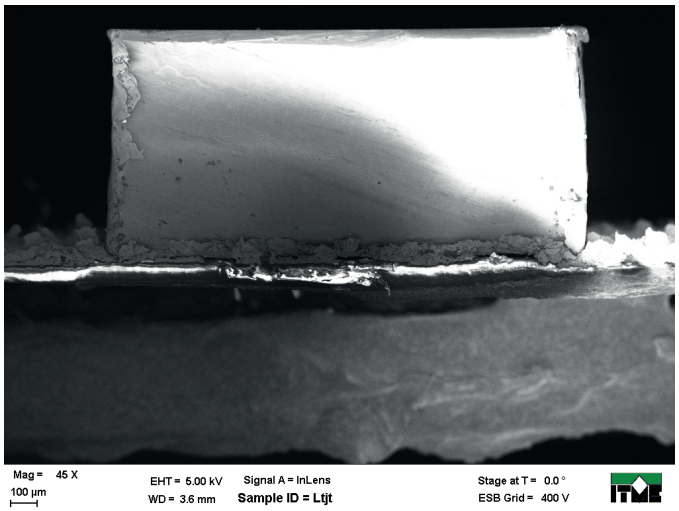

Fig. 9. SEM picture of the side of joined die

It can be observed in Fig. 11 that at the surface of the die the silver flakes are oriented horizontally and stick to the die's surface, which was the intended result of using silver flakes in addition to silver nanopowder. The thickness of a sintered joint was around 45 microns.

Porosity of the joint was measured by X-Ray tomography. Series of pictures were taken from the side of the sample, one picture per every 5 microns of depth. The cross-section of the top view of the sample is presented in Fig. 9. Porosity and the properties of pores was evaluated by means of using image recognition software. Due to the limited resolution of X-Ray tomography, only objects larger than 4x4 um were counted. The calculated values of porosity and electrical properties are collected in Table 3.

5. Conclusions

The method of bonding dies with bottom metallization to many rigid substrates and flexible polyimide foil has been presented. The paste containing silver nanoparticles allows to obtain superior electrical and thermal conductivity as compared to the other methods using die attach. The estimated electrical

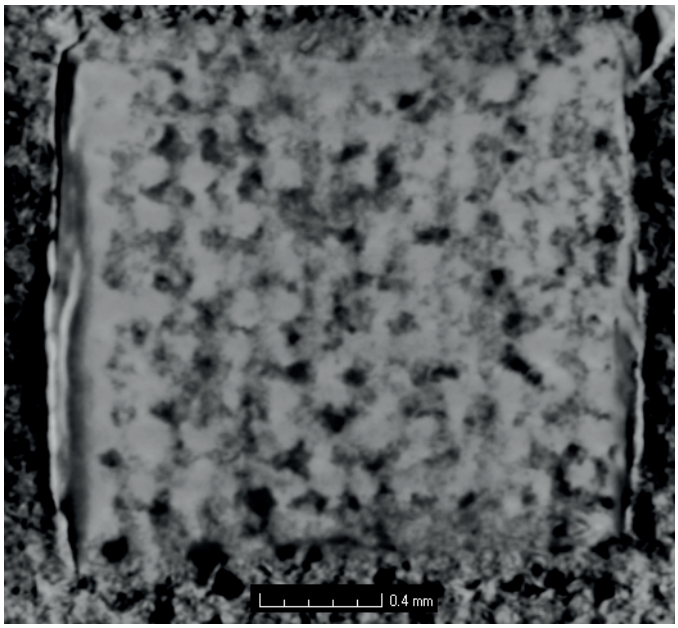

Fig. 10. Cross section of test structure taken by X-Ray tomography

conductivity is about 3 times higher than for the SnPb solder and about 9 times higher than for conductive adhesives. The joining is conducted by printing a silver based paste and then by the thermocompression method with 2.5 MPa of pressure at 300°C. Due to utilization of silver nanoparticles, the required joining pressure is 4 times lower than for the commercially available pastes. Low joining pressure allows to join stress-sensitive active and passive components starting from LED SMD0805 components up to 5×5 mm structures represented by joining the photovoltaic module. Unlike solders, the sintered layer contains 17% of porosity that, at the expense of slight decrease of electrical and mechanical properties as compared to bulk silver, enhances joint elasticity to the point where it can withstand about 10 000 cyclic stress changes between $\sigma = 0$ Pa and 18 MPa. This is essential for soft electronic circuits, where rigid components are joined to a flexible substrate. Additionally, the paste meets the requirements of the RoHS Directive.

Acknowledgement. This work has been partially financed by NCBiR, project No. UOD-DEM-1–215/001.

References

[1] R.A. Amro, "Packaging and interconnection technologies of power devices, challenges and future trends", *World Academy of Science, Engineering and Technology* Vol. 49, 2009.

[2] R. Kisiel and Z. Szczepański, "Die-attachment solutions for SiC power devices", *Microelectronics Reliability* 49, 627–629, 2009.

[3] C. Goebl and J. Faltenbacher, "Low temperature sinter technology die attachment for power electronic applications", *CIPS 2010*, (2010).

[4] F. Le Henaff, S. Azzopardi, E. Woirgard, T. Youssef, S. Bontemps, and J. Joguet, "Lifetime evaluation of nanoscale silver sintered power modules for automotive application based on experiments and finite-element modeling", *IEEE Transactions on Device and Materials Reliability* 15 (3), 326- 334, (2015).
[5] J.S. Hwang, "Overview of lead-free solders for electronics & microelectronics", *Proc. SMI 94 Conf.* , 405 (1994).
[6] T. Zhou, T. Bobal, M. Oud, and J. S. Coining „Au/Sn solder alloy and its applications in electronics packaging", http:// www.ametek-ecp.com/~/media/ametek-ecp/files/cwtechnicalpapers/coining_english_gold_tin_paper.pdf.
[7] http://buyersguide.pennwell.com/Shared/User/cyad09bd57558b-4f6a899c35f475a7af10.pdf.
[8] J. Szałapak, K. Kiełbasiński, J. Krzemiński, A. Młożniak, E. Zwierkowska, R. Pawłowski, and M. Jakubowska, "Method of calculating thermal diffusivity and conductivity for irregularly shaped specimens in laser flash analysis", *Metrol. Meas. Syst. XXII*, No. 4, 521–530, 2015.
[9] K. Kiełbasiński, J. Szałapak, M Jakubowska, A. Młożniak, E. Zwierkowska, J. Krzemiński, and M. Teodorczyk, "Influence of nanoparticles content in silver paste on mechanical and electrical properties of LTJT joints", *Advanced Powder Technology* 26 (3), 907–913, 2015.
[10] K.S. Siow, "Mechanical properties of nano-silver joints as die attach materials", *Journal of Alloys and Compounds* 514, pp. 6–19, 2012.
[11] Z. Zhang and G.-Q. Lu, "Pressure-assisted low-temperature sintering of silver paste as an alternative die-attach solution to solder reflow", *IEEE Transactions on Electronics Packaging Manufacturing* 25 (4), 2002.
[12] M. Maruyama, R. Matsubayashi, H. Iwakuro, S. Isoda, and T. Komatsu, "Silver nanosintering: a lead-free alternative to soldering", *IEEE Transactions on Electronics Packaging Manufacturing*, 25(4), 2002.
[13] S. Sakamoto and K. Suganuma, "Low temperature die-bonding with Ag flakes", EMPC 2011, (2011).
[14] M. Knoerr and A. Schletz, "Power semiconductor joining through sintering of silver nanoparticles: Evaluation of influence of parameters time, temperature and pressure on density, strength and reliability", CIPS 2010, Nuremberg, Germany, (2010).
[15] S. Hausner, S. Weiss, B. Wielage, and G. Wagner, "Joining of copper at low temperatures using Ag nanoparticles: Influence of process parameters on mechanical strength", *International Brazing & Soldering Conference*, Long Beach, (2015).
[16] C. Buttay, A. Masson, J. Li, M. Johnson, M. Lazar, C. Raynaud, and H. Morel, "Die attach of power devices using silver sintering – bonding process optimisation and characterization", HiTEN, (2011).
[17] S. Fu, Y. Mei, X. Li, P. Ning, and G. Q. Lu, "Parametric study on pressureless sintering of nanosilver paste to bond large- area (>100 mm^2) power chips at low temperatures for electronic packaging", *J. Electron. Mater*. 44 (10), 3973–3984, 2015.
[18] W. Schmitt, "New silver contact pastes from high pressure sintering to low pressure sintering," *3rd Electronic System-Integrated Technology Conference* (ESTC), Berlin, 2010.
[19] M. Jakubowska, M. Jarosz, K. Kiełbasinski, and A. Młożniak, "New conductive thick-film paste based on silver nanopowder for high power and high temperature applications", *Microelectronics Reliability* 51 (7), 1235–1240, 2011.
[20] http://silvercon.com.pl/en
[21] S. Paknejad, G. Dumas, G. West, G. Lewis, and S. Mannan, "Microstructure evolution during 300°C storage of sintered Ag nanoparticles on Ag and Au substrates", *J. Alloy Compd*. 617, 994–1001, 2014.
[22] Y. Fang, R.W. Johnson, and M.C. Hamilton, "Pressureless sintering of microscale silver paste for 300 C applications," *IEEE Trans. Compon. Packag. Manuf. Technol*. 5 (9), 1258–1264, (2015).